Dynamics of non-equilibrium charge carriers in p-germanium doped by gallium

Deßmann, N.; Pavlov, S. G.; Tsyplenkov, V. V.; Orlova, E. E.; Pohl, A.; Shastin, V. N.; Zhukavin, R. K.; Winnerl, S.; Mittendorff, M.; Klopf, J. M.; Abrosimov, N. V.; Schneider, H.; Hübers, H.-W.;

Originally published:

February 2017

Physica Status Solidi (B) 254(2017)6, 1600803

DOI: https://doi.org/10.1002/pssb.201600803

Perma-Link to Publication Repository of HZDR:

https://www.hzdr.de/publications/Publ-24865

Dynamics of non-equilibrium charge carriers in p-germanium doped by gallium

Nils Deßmann [*,1], S. G. Pavlov[2], V. V. Tsyplenkov[3], E. E. Orlova[3], A. Pohl[1], V. N. Shastin[3,4], R. Kh. Zhukavin[3], S. Winnerl[5], M. Mittendorff[5,6], J. M. Klopf[5], N. V. Abrosimov[7], H. Schneider[5], and H.-W. Hübers[1,2]

[1] Department of Physics, Humboldt-Universität zu Berlin, Newtonstr. 15, 12489 Berlin, Germany
[2] Institute of Optical Sensor Systems, German Aerospace Center (DLR), Berlin, Germany
[3] Institute for Physics of Microstructures, Russian Academy of Sciences, Nizhny Novgorod, Russia
[4] Nizhny Novgorod State University, Nizhny Novgorod, Russia
[5] Helmholtz-Zentrum Dresden-Rossendorf, Dresden, Germany
[6] Institute for Research in Electronics & Applied Physics, University of Maryland, USA
[7] Leibniz-Institute for Crystal Growth, Berlin, Germany

Received ZZZ, revised ZZZ, accepted ZZZ
Published online ZZZ (Dates will be provided by the publisher.)

Keywords Please provide about four verbal keywords for your manuscript.

* Corresponding author: e-mail nils.dessmann@dlr.de, Phone: +49 30 67055 7921, Fax: +49 30 67055 507

The low-temperature relaxation processes of non-equilibrium holes into gallium centers in moderately doped p-germanium ($N_A \approx 2\times10^{15}$ cm^{-3}) has been investigated by a degenerate pump-probe experiment using the free electron laser FELBE. The capture time decreases with increasing average photon flux density of the excitation pulse from about 10.9 ns (at ~1.2×10^{24} cm^{-2}s^{-1}) to ~1.2 ns (~2×10^{26} cm^{-2}s^{-1}). Relaxation inside the valence band is almost independent on pump light intensity and its characteristic time is about 200 ps. In Addition, the intracenter relaxation times of the lowest excited Ga states were measured. The lifetimes scale with the phonon density of states controlling a bound hole – acoustic phonon interaction. The lifetime of the lowest excited state, $1\Gamma_8^-$, was measured to be ~275 ps; while the lifetimes of the higher excited states, $2\Gamma_8^-$ and $3\Gamma_8^-$, were found to be ~157 ps and 162 ps, respectively.

1 Introduction Germanium doped with gallium (Ge:Ga) is a widely used semiconductor for sensitive low-temperature photon detectors of terahertz (THz) radiation at frequencies from approximately 1.5 THz to 6 THz (200–50 μm) [1, 2]. The high carrier mobility, low lattice absorption at THz frequencies and the possibility to precisely control of the doping make Ge a unique material for broadband and sensitive photodetectors. The most sensitive detection mechanism is based on photoconductivity induced by free charge carriers, which in turn are generated by absorption of THz radiation on transitions from the Ga ground state ($1\Gamma_8^+$) into the valence band (photo-ionization) and into excited Ga states (photoelectric excitation) (Fig. 1). The long-wavelength cutoff of these detectors is determined by the energy gap between the impurity ground state and the high odd-parity excited states in the vicinity of the valence band (VB). For Ge:Ga this corresponds to ~120 μm [1, 2]. It can be extended to ~200 μm by applying an uniaxial compressive force [3]. Spectrometers and photometers, which rely on these detectors, have been used in astronomy in a number of space- and airborne observatories. The most recent example is FIFI-LS, the Field-Imaging Far-Infrared Line Spectrometer. This spectrometer is equipped with two 16×25 pixel Ge:Ga detector arrays. One covers the range from 50 to 125 μm and the other one the range from 105 to 200 μm. Since 2014 it is in operation on SOFIA, the Stratospheric Observatory for Infrared Astronomy [4, 5].

Despite the wide use of this type of detector there is relatively little experimental evidence on the relaxation of photo-excited carriers into attractive Coulomb centers in n- and p-type Ge. While in n-Ge crystals interaction with in-

tervalley phonons can contribute to the large relaxation rates, in p-Ge crystals direct relaxation from degenerated light (*lh*) and heavy hole (*hh*) subbands with emission of an optical phonon can be expected. A detailed understanding of these processes is important, as they ultimately limit sensitivity and speed of such detectors.

For clarity, we shall denote the relaxation of a free hole from the valence band bottom into the ground impurity state as a capture process, the decay of a photo excited free hole within the valence band as intraband relaxation, and the relaxation of the bound charge carrier from excited into the ground Ga state as intracenter relaxation.

The low-temperature (T = 5–40 K) capture of free electrons in moderately doped n-Ge (Sb concentration ~1×10^{15} cm^{-3}) has been studied by a time-resolved pump-probe experiment at ~3 THz [6]. It revealed a typical capture time of approximately 1.7 ns. An additional intraband relaxation process with a characteristic time of approximately 200 ps occurs if electrons are excited above the bottom of the conduction band. This excitation can be achieved either by two-photon optical excitation, or, alternatively, by depopulation of the ground state due to elevated lattice temperature or electric impurity breakdown. Furthermore, the relaxation times of photo-excited free charge carriers in heavily doped (Sb and Ga concentration (2–5)$\times10^{16}$ cm^{-3}) and highly compensated Ge was studied [7]. The dominant dopant was either Ga (n-Ge:Ga:Sb) or Sb (p-Ge:Sb:Ga) with compensating doping levels close to 100 %. Compensation results in a larger number of attracting centers for photo-excited electrons, and by this, enhances the capture process. The relaxation time is a function of pump pulse energy and compensation and ranges from 30 to 300 ps. A fast photoconductive detector made from this material shows a response time of 150 ps which in the order of its fundamental relaxation time [7].

In this paper we present the time-resolved investigation of different relaxation mechanisms of photoexcited and photoionized carriers in p-Ge crystals moderately doped with Ga (~2×10^{15} cm^{-3}) with a low compensation (below 1 %). The measurements were performed with a dedicated pump-probe setup [8] at the free electron laser (FEL) FELBE of the Helmholtz-Zentrum Dresden-Rossendorf. In addition, the lifetimes of three bound excited states were measured by this method.

2 Sample characterization and measurement details The p-Ge:Ga crystal was Czochralski-grown and doped from the melt. A p-Ge:Ga sample with dimensions of 10×10×1 mm³ cut from this crystal was used for the measurement. It was wedged to an angle of ~ 0.5° in order to avoid light interference in the sample. Low-temperature absorption spectra were recorded with a Bruker Fourier transfrom infrared spectrometer (FTIR) Vertex 80V. For this purpose the sample was placed in a Janis ST-100-FTIR liquid helium (He) flow-cryostat and the temperature was measured with a Lakeshore Model 331 temperature controller on a sensor mounted on the cold finger in vicinity to the sample. The temperature was varied between 5 K and 60 K with a resistive heater attached to the sample holder. The strongest impurity transitions observed in the absorption spectra are between the ground state ($1\Gamma_8^+$) and the lower excited states ($1\Gamma_8^-$, $2\Gamma_8^-$ and $3\Gamma_8^-$), labeled in accordance with Ref. [9] as G, D and C, respectively (Figs. 1, 2). This confirms Ga centers to be the dominant dopant species. In Fig. 1 we choose the common energy zero position at the maximum (bottom) of the VB. Then, the bound Ga states, lying in the energy bandgap, have positive values of binding energies with the Ga ground state having an ionization energy of 11.32 meV. The optical depth (Fig. 1) is a product σdN, where σ is the absorption cross section, d is the sample's thickness, and N is the number density of absorption centers. The optical depths range from almost zero below photon energies corresponding to the G-line to about 4.5 at the maximum of the D-line (Fig. 1).

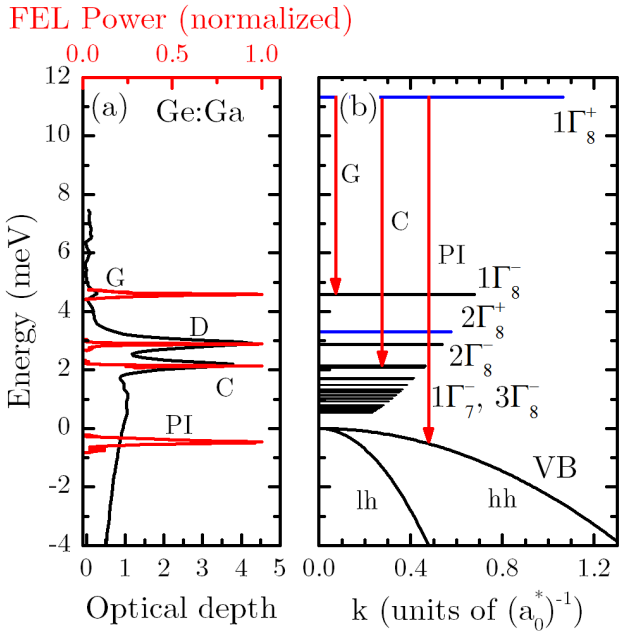

Figure 1 **(a)** Absorption spectrum of the investigated Ge:Ga sample (black line) and normalized FEL output spectra at the photon energies of the investigated transitions (red lines). The energy scale is set to zero at the Γ-point of the valence band. The spectral features correspond to intracenter transitions (indicated by G, D and C) [9]. **(b)** Energy diagram for Ge:Ga with FEL excitation transitions, wavenumber k is in units inversed to the effective Bohr radius a_0^*. Discrete energy levels of Ga acceptors in Ge [10] lie in the Ge bandgap; electronic states in vicinity of the minimum of the valence band are degenerated in the light (lh) and heavy hole (hh) subbands [9]. The red arrows down indicate photo-ionization (PI) and photo-excitation by FEL radiation at wavelengths of 105 µm (PI), 135 µm (C), 150 µm (D), and 184 µm (G).

To investigate the absorption processes in the Ge:Ga sample, we measured the temperature dependent absorption spectra between 5 K and 60 K in temperature steps of ~2.5 K (Fig. 2). The

occurrence of more than one absorption process leads to the superposition of their optical depths, $\sum_j \sigma_j dN_j$. Assuming constant σ_j's at a certain FEL wavelength λ_{FEL}, each absorption process can be seen as a measure of the number of the respective absorption centers N_j. For further comparison the optical depth was normalized for each temperature.

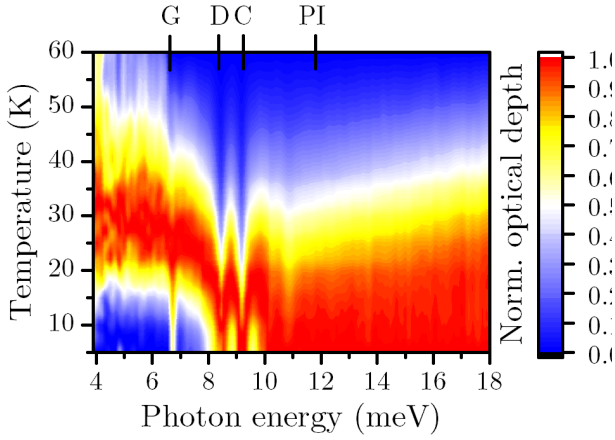

Figure 2 Absorption spectra of the investigated Ge:Ga sample at different temperatures from 5°K to 60°K. The spectra are normalized on maximal optical depth for each temperature.

At photon energies below the G-line (< 6 meV) the optical depth peaks at about 30 K and disappears for temperatures above 50 K. This indicates the existence of (*lh*-*hh*) inter-valence-band absorption and absorption on transitions between high excited Ga states, which arise from thermal excitation of the Ga centers. At higher photon energies this maximum shifts to lower temperatures and peaks when the FEL wavelength is in resonance with one of the intracenter lines.

For measuring the capture time when the carrier is excited into the valence band the λ_{FEL} was 105 µm (Fig. 1a). This corresponds to a photon energy (11.79 meV), larger than the ionization energy of the Ga centers, and it fits to an atmospheric window. For intracenter excitation the experiment was repeated with the λ_{FEL} that match the G- ($1\Gamma_8^+ \rightarrow 1\Gamma_8^-$), D- ($1\Gamma_8^+ \rightarrow 2\Gamma_8^-$), and the C-line ($1\Gamma_8^+ \rightarrow 3\Gamma_8^-$) at 184 µm (6.74 meV), 150 µm (8.27 meV), and 135 µm (9.18 meV), respectively. The pump-probe experiment is based on the time-resolved measurement of photoinduced transmission change, ΔT, of the sample. In the case of Ge:Ga this is caused by a non-equilibrium carrier population. The change in transmission as a function of the time delay between exciting (pump) and analyzing (probe) beams is a measure of the dynamics of the system towards equilibrium. In the experiment the incoming FEL radiation is split into a strong pump pulse and a weaker probe pulse using a Mylar beam splitter. The time delay of the probe pulse with respect to the pump pulse was realized with an optical delay stage in the probe beam path. FELBE provides pulses at a repetition rate of 13 MHz in a quasi-continuous mode and, hence, allows for the use of lock-in detection. The pump-probe signal (PPS), i.e. the pump-induced change of the probe beam transmitted through the sample, is measured by modulating the pump beam and recording the signal of the probe beam with a silicon bolometer. The mechanical chopping frequency in the pump beam path was set to ~360 Hz. Due to absorption by water in the probe beam path the signal has a systematic drift caused by the variation of the optical path length during the optical delay stage drive. This effect is compensated using a reference signal obtained by blocking the pump beam in front of the sample and measuring the lock-in signal of the modulated probe beam. The relative change in transmission of the sample induced by the pump, $\Delta T/T$, is obtained by dividing the PPS and the reference signal. This will be referred to as "relative PPS" in the text. For the measurements the sample was placed in a liquid He flow-cryostat and cooled to about 5 K, in order to ensure that the holes are bound to the ground state of the Ga centers. The cryostat was equipped with wedged diamond windows which have a flat transmission over the whole frequency range necessary for our measurements.

At the wavelengths of our experiments (105 µm, 135 µm, 150 µm, and 184 µm) the pulses are quasi-Gaussian shaped with a full width at half-maximum (FWHM) ranging from ~10 ps at 105 µm to ~18 ps at 184 µm. Pump and probe beams were focused onto the sample using a 10 cm focal-length off-axis parabolic mirror down to a spot of ~400 µm in diameter. They are slightly tilted (~10°) with respect to each other. The average FEL power was measured with a pyroelectric powermeter (Ophyr). Using the average power, spot size, pulse duration, reflection losses at the vacuum window and sample surfaces the average photon flux density of the pump pulse, Φ_{pump}, was estimated. Φ_{pump} was varied over a large range from 1.2×10^{24} cm^{-2}s^{-1} to 4.2×10^{26} cm^{-2}s^{-1}. The maximum average pump power available from the FEL in this experiment was 0.54 W, which corresponds to Φ_{pump} ~2.1×10^{26} cm^{-2}s^{-1}. It could be reduced with two sets of the diffractive attenuators in steps of 3 dB, 5 dB, and 10 dB. The probe power was kept constant at ~1.2×10^{24} cm^{-2}s^{-1} (average power ~2 mW).

3 Capture of photo-ionized carriers Previous investigations on n-Ge:Sb revealed a considerable contribution of intraband absorption in a pump probe experiment of up to 20 % due to a high population of the conduction band with non-equilibrium carriers at large Φ_{pump}. This ultimately leads to a bi-exponential temporal dependence of the measured PPS, especially at large Φ_{pump} [10]. Inter-valence-band transitions from the *lh*-subband to the *hh*-subband become considerably strong, if the light intensity is larger than ~1 MWcm^{-2} [11]. According to Ref. [12] absorption coefficient for transitions from the *hh* to the *lh* subband, α_{hl}, can be estimated as follows:

$$\alpha_{hl} = 8.25 T_l \sqrt{\lambda_{FEL}}\, e^{(\mu-0.125)/k_B T}. \qquad (1)$$

Here T_l is the lattice temperature in [K], k_B is the Boltzmann constant, λ_{FEL} in [µm], and μ is the chemical potential in [meV]. The equilibrium absorption cross section can then be obtained by dividing α_{hl} by the equilibrium hole concentration in the *hh* subband [12]. For typical values (T = 5 K, $N_A = 2\times10^{15}$ cm^{-3}, λ_{FEL} = 105 µm) the α_{hl} is about one order of magnitude larger than the indirect intra-conduction-band absorption cross section in the case of n-Ge:Sb. It contributes with about 50% to the total absorption cross section of p-Ge:Ga. A strong Φ_{pump} causes a large number of ionized Ga centers, N_i. By two-photon optical excitation, a fraction of the non-equilibrium carriers at the VB edge will be further excited by inter-valence-band absorption to the *lh* subband. The scattering of hot holes, N_h, from the *lh*-subband to the *hh*-subband is given by [13, 14]:

$$\tau_{lh}^{i} = -\frac{2^{3/2} m_l \varepsilon^2}{3\pi e^4 N_i} \frac{|E|^{3/2}}{m_h^{1/2}} \left(2 + \phi \ln\frac{\phi-1}{\phi+1}\right)^{-1}, \qquad (2)$$

with $\phi = \frac{1+m_h/m_l}{2\sqrt{m_h m_l}}$, m_h and m_l are the effective mass of holes in the *hh*- and in the *lh*-subband, correspondingly, ε is the dielectric permittivity, and $|E|$ is the hole's energy with respect to the bottom of the valence band (here $|E|$ ~12 meV for λ_{FEL} = 105 µm). The scattering rate of this process is estimated to be about 2×10^{11} s^{-1} and dominates the relaxation in the first few ps after excitation with a FEL pulse. The majority of hot holes will, therefore, relax to the *hh*-subband by the emission of acoustic phonons. This process can be estimated by an approach which is described in Ref. [15]. For a hole energy $|E|$ = 12 meV, which is approximately the ionization energy of the impurity centers, a *hh*-intraband relaxation rate of $(4–8)\times10^9$ s^{-1} is obtained at temperatures from 5 to 10 K. The latter corresponds to the intraband relaxation time τ_h ~ 125-250 ps.

We have measured the relative PPS at λ_{FEL} = 105 µm (11.8 meV) as a function of Φ_{pump}. In Fig. 3 three relative PPS of the Ge:Ga sample are shown for low (1.2×10^{24} cm^{-2}s^{-1}), medium (2.2×10^{25} cm^{-2}s^{-1}), and high (2×10^{26} cm^{-2}s^{-1}) Φ_{pump}. In order to obtain the characteristic time constants of both effects, hole capture and intraband relaxation, we fit the measured relative PPS, $\Delta T/T$, with a function *S(t)*, which is a convolution of the Gaussian-shaped probe pulse *exp(-(t-t$_0$)^2/(2Δt^2)), here Δt* is the Gaussian RMS width of the probe pulse and t_0 is the time of maximum overlap between pump and probe pulses, with the probe transmission through the sample. The transmission is determined by the population of the valence band bottom, $N_i(t) \sim exp(-t/\tau_c)$, and the hot hole concentration $N_h(t) \sim exp(-t/\tau_h)$. Here $\tau_c = \tau_c(N_i^0)$ is the capture time, $N_i^0 = N_i(0)$,, and τ_h is the intraband relaxation time of hot holes down to the bottom of the valence band. Furthermore, a third component in the relative PPS with a characteristic time τ_a, sensitive to the alignment of the setup and primarily visible at large Φ_{pump}, had to be taken in to account. This effect is known in the literature as the "coherent artifact". It can be caused for instance by pump-induced phase gratings in the sample [16, 17]. The fit equation is then given by

$$S(t) = e^{-\frac{(t-t_0)^2}{2\Delta t^2}} * \left(a \cdot e^{-\frac{t}{t_c}} + b \cdot e^{-\frac{t}{t_h}} + c \cdot e^{-\frac{t}{t_a}}\right) \qquad (3)$$

Here *Δt, t$_0$, a, b, c, τ$_c$, τ$_a$, τ$_h$* are fit parameters.

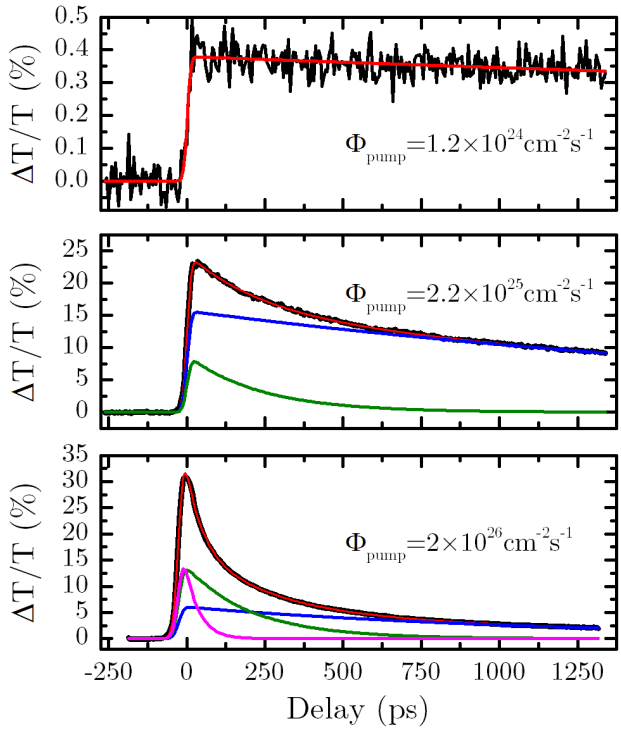

Figure 3 Pump-probe signals (black lines) of the Ge:Ga sample obtained at λ_{FEL} = 105 µm, Φ_{pump} of 1.2×10^{24}, 2.2×10^{25} and 2×10^{26} cm^{-2}s^{-1}. The red lines are fits with Eq. (3). The temperature of the sample was ~5°K. The blue, magenta and green lines are mono-exponential contributions to the relative PPS obtained from the fit. They show two processes, which are ascribed to intraband relaxation (green line) and hole capture by ionized centers (blue line). At low pump intensity, a mono-exponential fit (red = blue) is sufficient. At large Φ_{pump} (lowest graph) the signal is fitted with three components, the third component (magenta) is ascribed to the coherent artifact.

At low Φ_{pump} = 1.2×10^{24} cm^{-2}s^{-1} (top graph in Fig. 3) the signal can be fitted with a mono-exponential function with τ_c = 11 ns. This process is the capture of holes by ionized centers. As Φ_{pump} is increased to 2.2×10^{25} cm^{-2}s^{-1} a two-exponential fit is required (middle graph in Fig. 3). The main contribution (about 66 % of the total PPS) is the hole capture but with a much shorter characteristic time: τ_c ~3 ns. The second contribution of the PPS contributes about 33% to the total signal. The characteristic time is ~200 ps. This can be assigned to intraband relaxation. By going to higher $\Phi_{pump} = 2\times10^{26}$ cm^{-2}s^{-1} (bottom graph in Fig. 3) τ_c drops to ~1 ns. At this high photon flux the photo-induced occupation of the valence band is so large, that the

intraband relaxation dominates with about 66 % of the total PPS (excluding the contribution of the coherent artifact to the total signal). The characteristic time of the intraband relaxation is within the measurement uncertainty independent of Φ_{pump} and has a value of about 200 ps.

The main recombination mechanism in moderately doped and low compensated germanium at low temperatures is the cascade capture via emission of acoustic phonons. The characteristic energy of an acoustic phonon is much smaller than the binding energy, thus excited carriers relax gradually through the ladder of excited impurity states. The model of cascade capture was originally developed for isolated Coulomb centers [18]. The centers can be regarded as isolated when their concentration is relatively low and the orbitals, which are significant for the capture process, do not overlap. In this case the capture time is inversely proportional to the concentration of impurity ions. This in turn is proportional to the pump rate, provided the pump rate is low. The dependence of the capture time on Φ_{pump} is shown in Fig. 4. Up to $\Phi_{pump} \approx 4\times10^{25}$ cm^{-2}s^{-1} it is inversely proportional to the pump rate while above that value the dependence of the capture time on the pump rate is less pronounced. According to the cascade capture theory the capture time is proportional to $N_i^{-1/6}$ for densely spaced ionized centers, i.e. if the orbits relevant for the capture process overlap. This explains qualitatively the dependence of capture times at high pump rates.

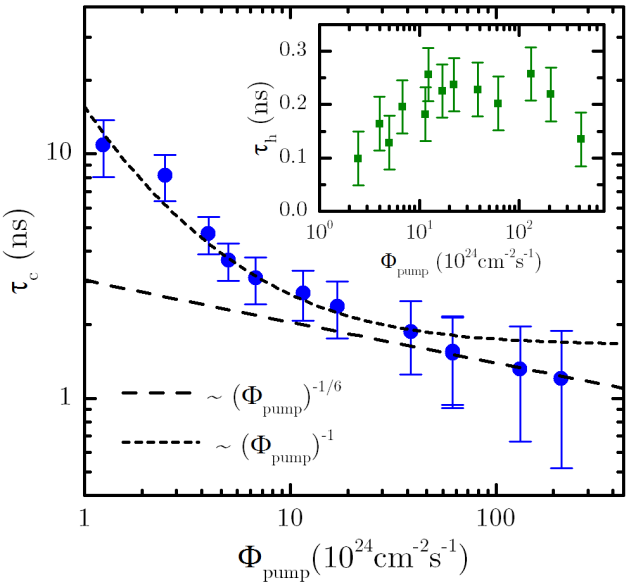

Figure 4 Capture time τ_c as a function of the photon flux density Φ_{pump}, λ_{FEL} = 105 µm: experimental results and fits according to the cascade capture via emission of acoustic phonons with account of overlap of the orbits of capture centers. Inset: dependence of intraband relaxation time τ_h on Φ_{pump}.

Figure 5 shows the peak value of the total PPS as well as the peak values of its two components for different Φ_{pump}. The change of transmission of the maximum of the total PPS, increases with Φ_{pump} from 0.4 % to 43 %. At large Φ_{pump} the modulation starts to saturate and peaks at 6.2×10^{25} cm^{-2}s^{-1} with 43 %. Above $\Phi_{pump} = 6.2\times10^{26}$ cm^{-2}s^{-1} the modulation drops rapidly apparently due to heating of the sample that decreases the Ga ground state population. The modulations related to impurity-to-band absorption, $\Delta T_{max,1}/T$, as well as to (*hh-lh*) inter-valence-band absorption, $\Delta T_{max,2}/T$, show a similar dependence on the pump rate. However, the maximum of the modulation for (*hh-lh*) inter-valence-band absorption is at higher pump rate while for impurity-to-band absorption it is at lower pump rate, because the first one requires a significant amount of holes in the valence band. This leads to the dominance of the (*lh-hh*) inter-valence-band absorption at Φ_{pump} larger than ~1×10^{26} cm^{-2}s^{-1}.

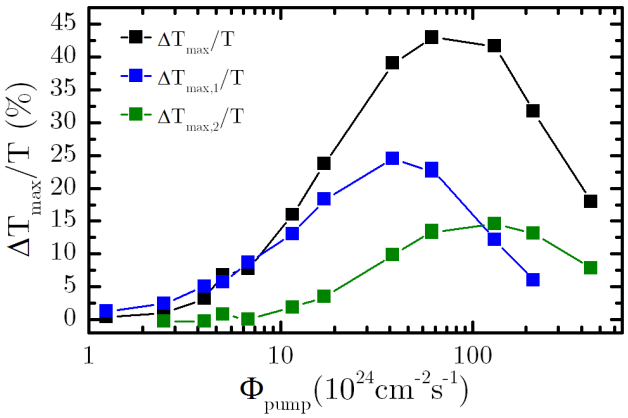

Figure 5 Dependence of the maximum of the relative transmission $\Delta T_{max}/T$) on the pump pulse energy at λ_{FEL} = 105 µm. They show the contributions of two processes to the decay of the relative PPS, namely intraband relaxation T_2 (green line) and hole capture by ionized centers T_1 (blue line). $T = T_1 + T_2$.

We summarize a five step photoionization-recombination process for non-equilibrium carriers in p-Ge (Fig. 6) with following derived relaxation rates: (1) Neutral Ga centers are ionized by the FEL radiation and holes are generated in the *hh* valence subband. (2) Subsequent excitation by *hh-lh* absorption transitions occurs, clearly detectable when reaching a critical carrier concentration in the *hh* valence subband (3) The scattering between *lh* und *hh* subband is very efficient (rate estimate 2×10^{11} s^{-1}) and leads to the population singularity in the *hh* subband at about twice the photon excitation energy with respect to the impurity ground state. (4) The relaxation down the *hh* subband by emission of acoustical phonons occurs on a typical time scale of ~200 ps (fixed rate 5×10^{9} s^{-1}). (5) The cascade capture into the Coulomb potentials of the ionized hydrogenic centers is the last step to the impurity ground state (rates are excitation power dependent, > 10^{8} s^{-1}). It is important to note that only a fraction of the ionized holes will pass the complete process. Depending on the degree of ionization a number of carriers will be directly captured by

the ionized center (5) after being pumped into the *hh* subband (1), omitting the steps (2) to (4).

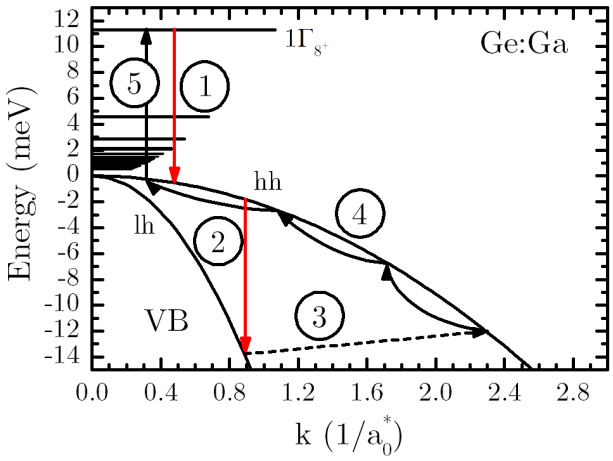

Figure 6 Five step photoionization-recombination processes as identified in the FEL pump-probe experiments for p-Ge:Ga. The subsequent two-step excitation from the impurity ground state $1\Gamma_8^-$ to the lh-subband (1, 2) is followed by lh-hh scattering (3) and intraband relaxation (4) with the final capture back to the ground state (5).

4 Intracenter recombination We measured lifetimes of the $1\Gamma_8^-$, $2\Gamma_8^-$ and $3\Gamma_8^-$ Ga states by setting the FEL to the G-line transition at 184 µm, the D-line transition at 150 µm, as well as to the C-line transition at 135 µm (Fig. 1). The spectral width of the FEL radiation was smaller than those of the Ga absorption lines. A component with a short time constant was present in all signals at wavelengths of 184 µm and 135 µm. We assign this component to the coherent artifact that was seen also in the measurements of the intraband relaxation processes at large Φ_{pump}. It is known that the width of the coherent artifact is similar to that of the incident pulse autocorrelation [19]. The fitting of the relative PPS was done according to Eq. (3), however, the fitting parameter τ_a in Eq. (3) was restricted to values below the pulse width to avoid any numerical interaction on the derived lifetimes.

At λ_{FEL} = 184 µm Φ_{pump} was varied over a range from 6×10^{24} to 5×10^{25} $cm^{-2}s^{-1}$. The relative PPS for Φ_{pump} = 5×10^{25} $cm^{-2}s^{-1}$ (Fig. 7a) shows the bi-exponential character of the signal. The longer time constant, assigned to the decay of the $1\Gamma_8^-$ state population, is independent on Φ_{pump} and has an arithmetic mean value of (275±59) ps (Fig. 7b). The FWHM duration of the FEL pulse derived from the fit was 18 ps in all PPS.

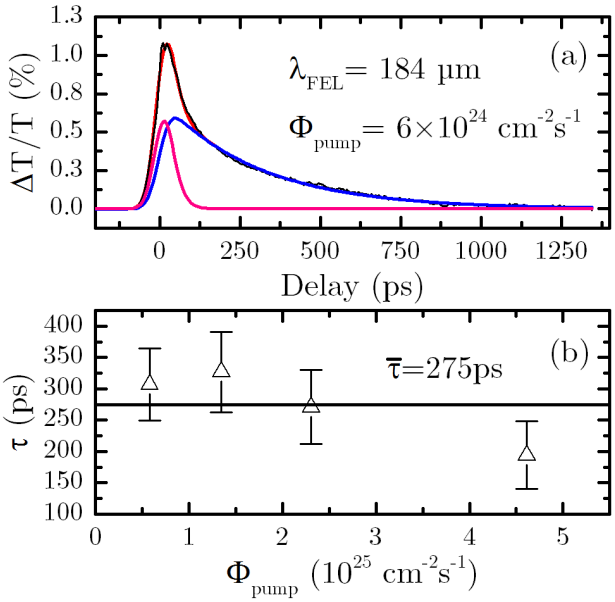

Figure 7 (a) Pump-probe signal (black line) of the Ge:Ga sample obtained at λ_{FEL} = 184 µm and Φ_{pump} = 5×10^{25} $cm^{-2}s^{-1}$. The red line is a fit with Eq. (3). The blue component of the bi-exponential fit is identified with the population decay of the $1\Gamma_8^-$ state. The magenta line is identified with the coherent artifact. **(b)** Lifetime τ of the $1\Gamma_8^-$ state as a function of Φ_{pump} obtained from the fit of the relative PPS. The arithmetic mean value $\bar{\tau}$ is 274 ps.

At λ_{FEL} = 150 µm Φ_{pump} was set to 2.5×10^{24} and 5×10^{24} $cm^{-2}s^{-1}$. In both cases only a mono-exponential signal was observed. A relative PPS for Φ_{pump} = 5×10^{25} $cm^{-2}s^{-1}$ is shown in Fig. 8a. The FWHM of the FEL pulse derived from the fit was ~18 ps in all relative PPS. The time constant of the population decay of the $2\Gamma_8^-$ state is consistent at both Φ_{pump} and shorter as the lifetime of the $3\Gamma_8^-$ state with a mean value of (157±41) ps (Fig. 8b).

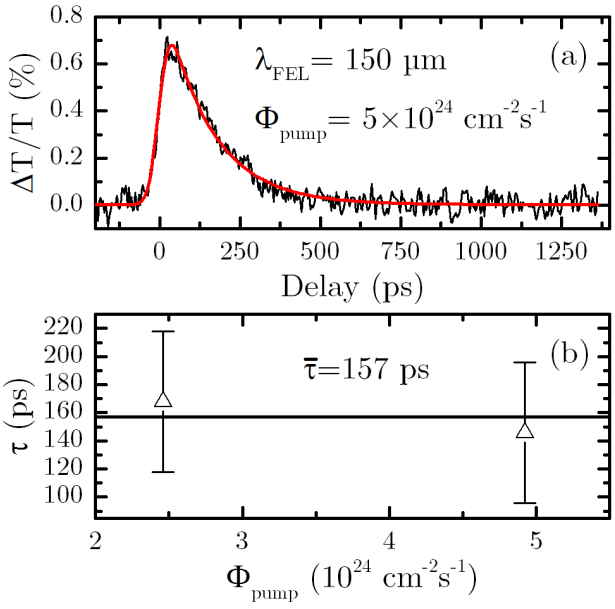

Figure 8 (a) Pump-probe signal (black line) of the Ge:Ga sample obtained at λ_{FEL} = 150 µm and $\Phi_{pump} = 5\times10^{24}$ cm^{-2}s^{-1}. The red line is a fit with Eq. (3). **(b)** Lifetime τ of the $2\Gamma_8^-$ state at two Φ_{pump} obtained from the fit of the pump probe signals. The arithmetic mean $\bar{\tau}$ is 157 ps.

At λ_{FEL} = 135 µm Φ_{pump} was varied from 3.2×10^{25} to 1×10^{26} cm^{-2}s^{-1}. A relative PPS for $\Phi_{pump} = 3.3\times10^{25}$ cm^{-2}s^{-1} is shown in Fig. 9a. Similar to the previous measurements we observed a bi-exponential relative PPS. Here the FWHM of the FEL pulse derived from the fit was ~13 ps in all relative PPS. The longer time constant which is identified with the population decay of the $3\Gamma_8^-$ state is independent on Φ_{pump}. The lifetime of the $3\Gamma_8^-$ state has a mean value of (162±37) ps (Fig. 9b).

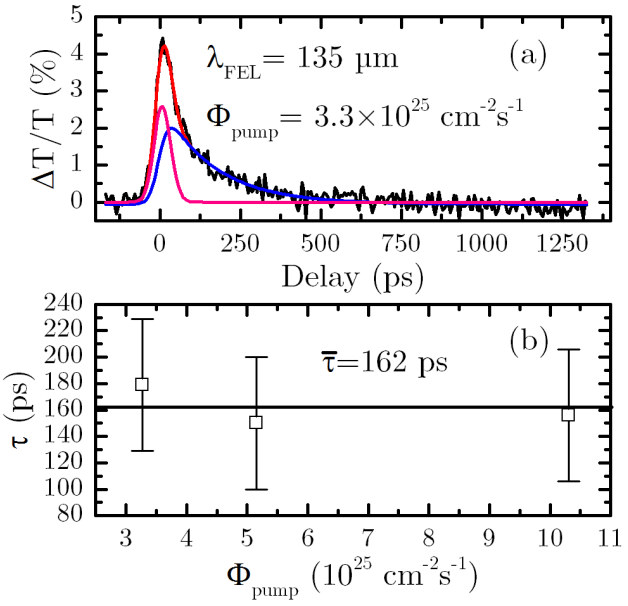

Figure 9 (a) Pump-probe signal (black line) of the Ge:Ga sample obtained at λ_{FEL} = 135 µm and $\Phi_{pump} = 3.3\times10^{25}$ cm^{-2}s^{-1}. The red line is a fit with Eq. (3). The blue component of the bi-exponential fit is identified with the population decay of the $3\Gamma_8^-$ state. The magenta line is identified with a coherent process. (b) Lifetime τ of the $2\Gamma_8^-$ state as a function of Φ_{pump} obtained from the fit of the pump probe signals. The arithmetic mean $\bar{\tau}$ is 162 ps.

As mentioned above, the cascade model describes the capture of free carriers by ionized centers as a sequence of small steps in energy space until the probability of thermal reemission into the continuum is practically zero [18, 20]. For p-Ge:Cu it has been confirmed experimentally that a considerable portion of the carriers is in bound excited acceptor states during the capture process [21]. The decrease of the probability of acoustic phonon assisted transitions with an increase of the transition energy is caused by the increase of the difference between the phonon momentum and the localization of impurity states in momentum space [22]. The energy gaps between the first excited states are the largest, thus implying the largest lifetimes for these states. On the other hand, comprehensive studies of both shallow acceptors [23] and donors [24] in silicon by using a time-resolving pump-probe setup and a FEL, support the presence of direct transitions from the excited states to the ground state. A correlation between the one-phonon density of states (PDOS) of silicon and phonon assisted relaxation rates was noted in [23]. In Fig. 10 the PDOS[25] of Ge is shown together with the absorption spectrum of the p-Ge:Ga sample. The G transition ($1\Gamma_8^- \rightarrow 1\Gamma_8^+$) is below the L_{TA} phonon resonance whereas the D and C transitions ($2\Gamma_8^-, 3\Gamma_8^- \rightarrow 1\Gamma_8^+$) are above that resonance; hence, the PDOS is larger. The $2\Gamma_8^-$ and $3\Gamma_8^-$ state are energetically above the $1\Gamma_8^-$ state and have an about 120 ps shorter lifetime, while at about the same PDOS their lifetimes are equal. In accordance with the measurements for silicon, we attribute the difference of the lifetimes of excited states in p-Ge to the PDOS (Fig. 10) which at higher values leads to a more efficient phonon-assisted relaxation.

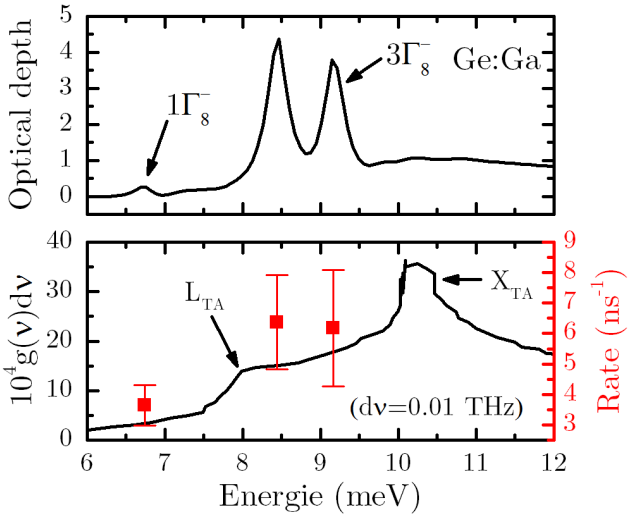

Figure 10 (a) Part of the absorption spectrum of the p-Ge:Ga sample, and **(b)** compared with the experimental relaxation rates and the PDOS [25] of Ge (80 K); arrows indicate energy of transversal acoustic (TA) phonons in Ge.

The lifetimes of Ga excited states which we have derived are order(s) of magnitude shorter than those reported for shallow acceptors in Ge in the experimental works. The calculated lifetime of the first excited state of an acceptor in Ge in Ref [22] is about 100 ns. Gershenzon *et al.* [26] have reported the lifetime of the $1\Gamma_8^-$ state in p-Ge:B to be as ~60 ns by analyzing line intensities of photoconductive spectra measured with a wide range of background illumination [27]. A theoretical analysis of acceptor quantum transitions supported this lifetime [26]. More accurate theoretical analysis of intracenter relaxation in p-Ge is desirable.

5 Conclusions We have measured the low-temperature capture of free holes into ionized Ga centers in moderately

doped p-Ge ($N_A \approx 2\times10^{15}$ cm^{-3}) using a single color pump-probe experiment and the free electron laser FELBE. The capture time decreases with increasing pump photon flux density from about 10.9 ns (at ~1.2×10^{24} cm^{-2} s^{-1}) to ~1.2 ns (~2×10^{26} cm^{-2} s^{-1}) due to an increase of the number of ionized impurity centers. We have shown that the capture rate is determined by the cascade model in the range of number of ionized impurity centers below 2×10^{15} cm^{-3}. With increasing pump power we observe a deviation from a sole cascade decay. The process with a characteristic time of ~200 ps is identified as an additional intraband relaxation process, caused by a subsequent excitation inside the valence band, similar to those previously observed for n-Ge:Sb [10]. Additionally, we have determined the lifetimes of the lowest $1\Gamma_8^-$ and the shallower $2\Gamma_8^-$ and $3\Gamma_8^-$ odd-parity excited states as 275 ps, 157 ps and 162 ps, respectively. In contrast to [22,27] we could not confirm the long lifetimes. With this a contribution of all excited states in the recombination process is imaginable. The $1\Gamma_8^-$ state has a binding energy below the L_{TA} phonon resonance, i.e. in a region with a smaller PDOS compared to the $2\Gamma_8^-$ and $3\Gamma_8^-$ states above that resonance. Hence, our measurements suggest a direct dependence of the excited states lifetimes on the PDOS that determines a bound hole – acoustic phonon interaction.

Acknowledgements This research has been funded by the joint German-Russian program "Research on technological advances of radiation sources of photons and neutrons based on accelerators and neutron sources in cooperation with research organizations and universities of the Federal Republic of Germany" (InTerFEL project, BMBF No. 05K2014 and the Russian Ministry of Science and Education, unique identifier No. RFMEFl61614X0008). N.D. and A.P. gratefully acknowledge support by the Helmholtz Research School on Security Technologies. We are grateful to P. Michel and the FELBE team for their dedicated support.

References

[1] E.E. Haller, Infrared Phys. Technol. **35**, 127 (1994).

[2] E. Bründermann, H.-W. Hübers, and M.F. Kimmitt, *Terahertz Techniques* (Springer Series in Optical Sciences, Berlin, Heidelberg, New York, 2012).

[3] A.G. Kazanskii, P.L. Richards, and E.E. Haller, Appl. Phys. Lett. **31**, 496 (1977).

[4] S. Colditz, F. Fumi, N. Geis, R. Hönle, R. Klein, A. Krabbe, L. Looney, A. Poglitsch, W. Raab, M. Savage, F. Rebell, and C. Fischer, in *Proc. SPIE*, edited by I.S. McLean, S.K. Ramsay, and H. Takami ({SPIE}, 2012), p. 844617.

[5] R. Klein, S. Beckmann, A. Bryant, S. Colditz, C. Fischer, F. Fumi, N. Geis, R. Hönle, A. Krabbe, L. Looney, A. Poglitsch, W. Raab, F. Rebell, and M. Savage, in *Proc. SPIE* ({SPIE}, 2014), p. 91472X.

[6] N. Dessmann, S.G. Pavlov, V.N. Shastin, R.K. Zhukavin, V. V. Tsyplenkov, S. Winnerl, M. Mittendorff, N. V. Abrosimov, H. Riemann, and H.-W. Hübers, Phys. Rev. B **89**, 35205 (2014).

[7] N. Deßmann, S.G. Pavlov, A. Pohl, N. V. Abrosimov, S. Winnerl, M. Mittendorff, R.K. Zhukavin, V. V. Tsyplenkov, D. V. Shengurov, V.N. Shastin, and H.-W. Hübers, Appl. Phys. Lett. **106**, 171109 (2015).

[8] S. Winnerl, M. Orlita, P. Plochocka, P. Kossacki, M. Potemski, T. Winzer, E. Malic, A. Knorr, M. Sprinkle, C. Berger, W.A. de Heer, H. Schneider, and M. Helm, Phys. Rev. Lett. **107**, 237401 (2011).

[9] A.K. Ramdas and S. Rodriguez, Reports Prog. Phys. **44**, 1297 (1981).

[10] N. Deßmann, S.G. Pavlov, V.N. Shastin, R.K. Zhukavin, V.V. Tsyplenkov, S. Winnerl, M. Mittendorff, N. V. Abrosimov, H. Riemann, and H.-W. Hübers, Phys. Rev. B - Condens. Matter Mater. Phys. **89**, (2014).

[11] S.D. Ganichev, S.A. Emel'yanov, E.L. Ivchenko, E.Y. Perlin, Y. V. Terent'ev, A. V. Fedorov, and I.D. Yaroshetskii, J. Exp. Theor. Phys. **64**, 729 (1986).

[12] Y.T.T. Rebane, Sov. Phys. -- Semicond. **14**, 289 (1981).

[13] D. Kranzer, Phys. Status Solidi **26**, 11 (1974).

[14] M.I. D'yakonov and A. V. Khaetskii, Zh. Eksp. Teor. Fiz **59**, 1072 (1984).

[15] M. Costato and L. Reggiani, Phys. Status Solidi **58**, 471 (1973).

[16] S.L. Palfrey and T.F. Heinz, J. Opt. Soc. Am. B **2**, 674 (1985).

[17] Z. Vardeny and J. Tauc, Opt. Commun. **39**, 396 (1981).

[18] V.N. Abakumov, V.I. Perel', and I.N. Yassievich, Zh. Eksp. Theor. Fiz **45**, 354 (1977).

[19] H. Liu, H. Zhang, J.-H. Si, L.-H. Yan, F. Chen, and X. Hou, Chinese Phys. Lett. **28**, 86602 (2011).

[20] M. Lax, Phys. Rev. **119**, 1502 (1960).

[21] I. Wilke, O.D. Dubon Jr, J.W. Beeman, and E.E. Haller, Solid State Commun. **93**, 409 (1995).

[22] S. V. Meshov and I. Rashba, J. Exp. Theor. Phys. **49**, 2206 (1979).

[23] N.Q. Vinh, B. Redlich, A.F.G. van der Meer, C.R. Pidgeon, P.T. Greenland, S.A. Lynch, G. Aeppli, and B.N. Murdin, Phys. Rev. X **3**, 11019 (2013).

[24] S.A. Lynch, P.T. Greenland, N.Q. Vinh, K. Litvinenko, B. Redlich, L. van der Meer, M. Warner, A.M. Stoneham, G. Aeppli, C.R. Pidgeon, and B.N. Murdin, in *2008 5th IEEE Int. Conf. Gr. IV Photonics* (IEEE, 2008), pp. 24–26.

[25] G. Nelin and G. Nilsson, Phys. Rev. B **5**, 3151 (1972).

[26] E.M. Gershenzon, G.N. Gol'tsman, and N.G. Ptitsina, JETP Lett. **25**, 539 (1977).

[27] E.M. Gershenzon, G.N. Gol'tsman, and N.G. Ptitsina, J. Exp. Theor. Phys. **49**, 711 (1979).